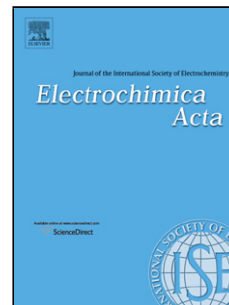


Accepted Manuscript

Title: C-OHbond cleavage initiated by electron transfer:
electroreduction of 9-fluorenol

Author: Andrey S. Mendkovich Mikhail A. Syroeshkin Darya
V. Nasybullina Mikhail N. Mikhailov Vadim P. Gulytai
Mikhail N. Elinson Alexander I. Rusakov



PII: S0013-4686(16)30129-3
DOI: <http://dx.doi.org/doi:10.1016/j.electacta.2016.01.127>
Reference: EA 26509

To appear in: *Electrochimica Acta*

Received date: 29-10-2015
Revised date: 27-12-2015
Accepted date: 17-1-2016

Please cite this article as: Andrey S.Mendkovich, Mikhail A.Syroeshkin, Darya V.Nasybullina, Mikhail N.Mikhailov, Vadim P.Gulytai, Mikhail N.Elinson, Alexander I.Rusakov, mC-OHbond cleavage initiated by electron transfer: electroreduction of 9-fluorenol, *Electrochimica Acta* <http://dx.doi.org/10.1016/j.electacta.2016.01.127>

This is a PDF file of an unedited manuscript that has been accepted for publication. As a service to our customers we are providing this early version of the manuscript. The manuscript will undergo copyediting, typesetting, and review of the resulting proof before it is published in its final form. Please note that during the production process errors may be discovered which could affect the content, and all legal disclaimers that apply to the journal pertain.

C-OH bond cleavage initiated by electron transfer: electroreduction of 9-fluorenol

Andrey S. Mendkovich^{a*}, Mikhail A. Syroeshkin^a, Darya V. Nasybullina^a, Mikhail N. Mikhailov^a, Vadim P. Gulyai^a, Mikhail N. Elinson^a, Alexander I. Rusakov^b

^aN. D. Zelinsky Institute of Organic Chemistry, Russian Academy of Sciences, 119991 Moscow, Russian Federation. Fax: +7 499 135 5328; e-mail: asm@free.net

^bP. G. Demidov Yaroslavl State University, 150000 Yaroslavl, Russian Federation

Graphical abstract

Highlights

- The electroreduction of 9-Fluorenol in aprotic media was studied.
- The process proceeds via C–O bond cleavage in the radical anion.
- The substrate is deprotonated by anionic products giving rise 9-fluorenone dianion.

Abstract

Cyclic voltammetry, chronoamperometry, coulometry, electrolysis, digital simulation, quantum chemical calculations of 9-fluorenol as an example, were used to show that the electroreduction of aryl derivatives of methanol in 0.1 M Bu₄NClO₄/DMF proceeds via the ECE mechanism (including the stages of radical anion formation and the C–OH bond cleavage in the radical anion) complicated by the reactions of the depolarizer with the anionic products. Among these reactions are the deprotonation of 9-fluorenol and its monoanions by hydroxide anion and fluorenyl anion. The thermodynamic parameters of the reactions have been estimated both theoretically and experimentally. It was found that the equilibrium constants of the fluorenyl anions deprotonation are close (C-anion) or higher (O-anion) than that of fluorenol. As a result the total equilibrium is shifted towards the side of the dianion of 9-fluorenone. The unusual ratio of the equilibrium constants was explained by lower basicity of π^* -dianion compare with other anions.

Keywords: 9-Fluorenol; cyclic voltammetry; chronoamperometry; radical anion; dissociative electron transfer.

1. Introduction

It is known that the presence of an electron on an antibonding molecular orbital destabilizes bonds, transfer of an electron to a neutral molecule could result in dissociation of the latter [1]. A considerable number of papers deal with studies on bond cleavage processes initiated by the electron transfer [2-9]. One of the main reasons of this special attention to these reactions is that they are of undoubted interest both for organic synthesis [10-13] and for theoretical organic chemistry, *e.g.*, in interpretation of results of experimental studies on nucleophilic substitution processes [14-17]. Furthermore, bond cleavage reactions in biological systems attracted the serious attention of researchers in recent years [18-21].

Many examples are known in literature for dissociation reactions of various types of bonds initiated by electron transfer resulting in elimination of various functional groups.

The following examples can be specially mentioned: elimination of nitrite anions from radical anions of nitroaromatic compounds [22-23], phenoxide anions [24] and benzoate anions [25] from radical anions of ethers and esters, arylsulfonate anions from the corresponding olephine derivatives [26] thiophenolate anions from triphenylmethane derivatives [27-28] and other derivatives [29], alkylsulfide anions from disulfide radical anions [30-31], alkoxy anions from radical anions of organic peroxides [32-46], substituted benzyl anions from radical anions of bicumenes [47] *etc.* The regioselectivity of bond cleavage in benzylthiocyanates (C-SCN or CS-CN) [48] and sulfenate esters (S-O or C-O) [49] depending on radical anion structure was discussed. Researchers paid particular attention to the elimination of a halide anion from radical anions of halogen derivatives, both aliphatic [50-56] and aromatic [57-62]. The reactions of radical anions of these compounds have been studied most thoroughly, both experimentally and theoretically [2, 3] [63]. This is primarily due to the fact that formation of radical anions of this class of compounds plays an important role in many reactions of practical interest, *e.g.*, in formation of Grignard reagents [64-67] and in electrochemical generation of carbenes [68].

On the other hand, only few papers are available in literature that describe the elimination of an OH group initiated by the electron transfer. Cleavage of an N-OH bond was observed in electroreduction of oximes [69] and N-arylhydroxylamines [70]. It was also shown [71] that electroreduction of methanol derivatives containing unsaturated and aromatic substituents in aprotic solvents could be described by the scheme:



An attempt to elaborate this scheme was made in subsequent studies [72-73]. However, the conclusions concerning the primary products of C-OH bond dissociation due to electron transfer were contradictory. For example, the mechanism proposed for electroreduction of 9-

hydroxybifluorenyl [72] involved a step of elimination of an OH radical from its radical anion, whereas the same researchers assumed elimination of a hydroxide anion from the radical anion of 9-fluorenyl $1^{\cdot-}$ with similar structure [73]. It also remained unclear whether dissociative electron transfer in the case of **1** and related compounds is a stepwise or synchronous process, since curves of cyclic voltammetry for compound **1** at potential scan rates up to $100 \text{ V}\cdot\text{s}^{-1}$ contained no anodic peaks corresponding to oxidation of its radical anion [73]. Likewise, no radical anion formation was detected in the reaction of 1,1-diphenylmethanol with solvated electron [74]. Therefore, we undertook an electrochemical and quantum-chemical study of C-OH bond cleavage initiated by electron transfer for compound **1** as an example.

2. Experimental

2.1. Electroanalytical and electrolysis instrumentation, experimental techniques and reagents

Chronoamperometry (CA), cyclic voltammetry (CV), coulometry and controlled potential electrolysis were implemented on an IPC-Pro computer-assisted potentiostat manufactured by Econix (potential scan rate error 1.0%; the potential is set to within 0.25 mV). Experiments were performed in a 10-mL five-neck glass conic electrochemical cell with a water jacket for thermostating. Polarization curves were recorded using a three-electrode scheme. The working electrode was a glassy-carbon disc electrode ($d = 1.7 \text{ mm}$). A graphite rod was utilized as a cathode for the coulometry and electrolysis. A platinum wire (insulated by a ceramic membrane in coulometry and electrolysis) served as the auxiliary electrode. A saturated calomel electrode (SCE) was used as the reference electrode and was connected to the solution by a bridge with a porous ceramic diaphragm filled with the background electrolyte (0.1 M Bu_4NClO_4 solution in DMF). The tested solutions were thermostatted at $25 \pm 0.5 \text{ }^\circ\text{C}$. Deaeration of solutions was performed by passing argon. To prevent the solution surface from contact with ambient air during the experiment, argon was constantly fed to the cell free space above the solution surface. In a typical case, 5 mL of a solution was utilized. The working electrode was polished and the solution was agitated vigorously with argon before recording each CA and CV curve.

To analyze CA and CV curves, the current values in the presence of the substrate were corrected for the current of the background electrolyte at this potential. The depolarizer concentration (C) was 2.5, 5, 7.5, 10, 15, 20, and $25 \text{ mmol}\cdot\text{L}^{-1}$. In the case of CV, the cathodic and anodic peak currents at the potential scan rates (ν) of 0.05, 0.1, 0.225, 0.4, 0.65, 1, 2 and $3 \text{ V}\cdot\text{s}^{-1}$ were used as response functions. The above-mentioned variations of C and ν correspond the change in the kinetic parameter λ [75-76] by more than four orders of magnitude. The sampled current voltammograms [77] (a subtype of steady-state voltammograms [78]) were

plotted using the values of the current from the CA curves at a transient time (t) of 4 s at the corresponding potentials. To compare the experimentally obtained and simulated CA curves, the values of the current at the potentials of the limiting current of the first wave in the sampled current voltammograms (i_{lim}^1) in the range of $t = 1\text{-}4$ s were used as the response function.

As the effects of uncompensated resistance (R_u) were significant in the present work, its value was measured accurately. The CV curves of ferrocene electrooxidation [79] were used for this purpose. R_u was calculated as the slope of the peak potential vs peak current plot for anodic and cathodic peaks from CV curves of 2.5, 5, 10, 15, 20, 25 and 30 mmol·L⁻¹ solutions of ferrocene at scan rates of 0.025, 0.05, 0.1, 0.225, 0.4, 0.65, 1, 2, and 3 V·s⁻¹. The resulting curves are strictly linear, and their slopes correspond to $R_u = 840 \pm 10 \Omega$. This value is specific to the working electrode used in this work and the arrangement of the electrodes in the cell, which was carefully reproduced in each experiment. The exact active area of the working electrode (equal to 2.30 mm²) was determined by simulation of the CV curves of ferrocene electrooxidation using the known ferrocene diffusion coefficient in DMF [80].

9-Fluorenone, 9-fluorene, 9-fluorenone, tetrabutylammonium perchlorate, tetrabutylammonium hydroxide, MeCN and DMF (“extra dry” grade) were supplied by Acros Organics.

100 mg of **1** was electrolyzed in MeCN at the potential -2.6 V vs SCE. After consumption of one mole equivalents of charge the electrolysis was stopped and catholyte was exposed to air to oxidize **3**²⁻ and the solvent was evaporated. Thin-layer chromatography on silica with hexane-ethyl acetate 12:1 as eluent revealed the presence in catholyte of two products: **2** ($R_{f, 2} = 0.76$) and **3** ($R_{f, 3} = 0.40$). No spot corresponding to **1** ($R_{f, 1} = 0.13$) was observed. The products separation by column chromatography on silica (0.04-0.063 mm) with hexane-ethyl acetate 12:1 as eluent gave **3** in 50% yield and **2** in 20%. Intensely colored layer of the insoluble in polar solvent material at the top of the column indicated the formation of the resins. The molecular ion peaks in mass spectra of the isolated compounds are 166 and 180 m/z, i.e. identical to those in spectra of **2** and **3**.

2.2. Digital simulations

Digital simulations of the CA and CV curves were carried out using DigiElch Professional, version 4.0 (Build 3.008), from ElchSoft. The computation of the model curves took into account the edge effect and uncompensated resistance. In case of CV curves of **1** the effect gives rise to changes in the current for low scan rates and long transient times up to 4% for cathodic peak and up to 19% for anodic peak corresponds to the oxidation of **3**⁻. The rate constants were determined from the CA and CV data using the procedure described previously

[70, 81] involving the variation of concentrations as well as scan rate or transient time in the case of CV and CA, respectively.

The diffusion coefficient D for **1** was taken to be $10^{-5} \text{ cm}^2 \cdot \text{s}^{-1}$. It was based on the value which we found for **3**, compounds structurally similar to **1**, whose anion radical is stable under these the conditions. In the case of **3**, the use of the value of $D = 10^{-5} \text{ cm}^2 \cdot \text{s}^{-1}$ enabled us to achieve a good agreement between the experimental (i_p) and theoretical (i_p^{theor}) first peak currents in the entire range of concentrations and potential scan rates studied. The mean ratio of peak currents was $i_p / i_p^{theor} = 0.99 \pm 0.03$.

The values of the transfer coefficients (α) were taken to be 0.5. Proton transfer reactions (4-10, 13 and 14) and rate constant of bond cleavage (2) considered to be fast. Theoretical values of the homogeneous equilibrium constants (K) have been used as the initial approximations. The standard potentials (E°) and heterogeneous electron transfer constants (k_s) as well as K magnitudes were determined by optimization using standard DigiElch Professional techniques to attain the best match of the model and the experimental curves over the ranges of potential scan rates and concentrations indicated above, followed by determination of the average values. The values was used for calculation of i_p^{theor} , and i_p / i_p^{theor} ratio was used to assess the overall quality of the results of the fitting process.

When optimizing it was taken into account that $K_4/K_5=K_7/K_6=K_9/K_{10}=K_{13}/K_{14}=K_{15}$ and, as it was found earlier [82], $K_9/K_5 = 1.5 \cdot 10^2$. In case of electroreduction of **3** in the presence of **2** the best agreement between simulation and the experimental voltammograms were obtained for the following set of simulation parameter: $E^\circ_{11} = -1.23 \text{ V}$, $E^\circ_{12} = -1.87 \text{ V}$, $K_6=9.5 \cdot 10^{-2}$, $K_{13}= 1.5$, $K_{15}=15.0$. The values were used in simulation of **1** electroreduction process to reduce the number of simulation parameters. The best coincidence with the experimental results in this case was attained when using the following values: $E^\circ_1 = -2.55 \text{ V}$, $K_4 = 9.6 \cdot 10^4$, $K_9 = 9.7 \cdot 10^5$, $K_{14} = 9.47 \cdot 10^{-2}$.

2.3. Quantum chemical calculations

The quantum chemical calculations were performed in the framework of density functional theory (DFT) using the B3LYP exchange correlation functional [83-85]. As we showed earlier [86], the calculated energies of the radical anions of compounds containing π -bonds depend fairly strongly on the presence of diffuse functions on hydrogen atoms in the basis set, whereas these effects are insignificant for compounds without π -bonds. Therefore, in this work, all calculations were performed using the 6-311++G(d,p) basis set. All quantum chemical calculations were performed using the Gaussian 03 [87] and Gaussian 09 [88] program packages.

Geometry optimization was carried out for all species under investigation. The character of the stationary points found (minimum or saddle point on the PES) was determined by calculation of the eigenvalues of the matrix of the second derivatives of energy with respect to nuclear coordinates. The influence of solvation was taken into account in all optimizations in the framework of the reactive field continuum model theories: PCM [89-91] and CSC-PCM [92], using the parameters for DMSO, which are similar to those of DMF that was used in the experiment. Energy profile (Fig. 1) for reaction (3) has been calculated by geometry optimized at fixed C-O distances. Equilibrium constants were calculated using Gibbs free energy values listed in the Table 1.

3. Results and discussion

3.1. Quantum chemical calculations

Figure 1 demonstrates the profile of $\mathbf{1}^{\cdot-}$ dissociation reaction obtained by calculation of its potential energy surface (PES). As one can see in Fig. 1, $\mathbf{1}^{\cdot-}$ in aprotic medium with a dielectric constant close to that of DMF can, in fact, exist as a kinetically independent species, as indicated by the corresponding minimum on its PES. Calculations show that the formation of $\mathbf{1}^{\cdot-}$ involves considerable structural changes. In particular, the C-O bond length increases by 0.06 Å and the C4a-C4b bond length decreases by 0.05 Å.

Though transfer of an electron to $\mathbf{1}$ gives the corresponding radical anion, the latter is thermodynamically and kinetically unstable and should decay to give a hydroxyl anion OH^- and fluorenyl radical $\mathbf{2}^{\cdot}$ (Fig. 1). The Gibbs free energy of $\mathbf{1}^{\cdot-}$ dissociation are $-18.9 \text{ kcal}\cdot\text{mol}^{-1}$. The activation energy calculated as the difference between energies of optimized structures of transition state and $\mathbf{1}^{\cdot-}$ equal $6.4 \text{ kcal}\cdot\text{mol}^{-1}$. The latter value is approximately two times smaller than the activation energy of dissociation of a carbon-halogen bond in aryl halide radical anions [93]. It is known [1] that the relatively high activation energies of the latter are due to the fact that the carbon-halogen bond lies in the plane of the aromatic system, hence its dissociation is forbidden for symmetry reasons. Therefore, the carbon-halogen bond should not only be elongated but should also deviate from the plane for this reaction to occur. As shown in [93], this deviation can be up to $\sim 30^\circ$ in the transition state and can decrease the activation energy 2-3 fold.

Unlike aryl halides, the hydroxy group that undergoes elimination in $\mathbf{1}^{\cdot-}$ is located outside the aromatic system plane, so there are no symmetry limitations for $\mathbf{1}^{\cdot-}$ dissociation. However, as one can see from Fig. 2, an increase in the length of the dissociating bond is also accompanied by considerable structural changes. It is interesting that the process that occurs in

this case is opposite to that observed for anion radicals of aryl halides, namely, planarity increases due to a change in C9 atom hybridization from sp^3 to sp^2 .

Thus, the results of quantum-chemical calculations make it possible to believe that the electron transfer to molecule **1** produces $\mathbf{1}^{\cdot-}$ (1), which decomposes to fluorenyl radical $\mathbf{2}^{\cdot}$ and a hydroxide anion (2). Quantum-chemical calculations show that the electron affinity of $\mathbf{2}^{\cdot}$ is 1.7 eV higher than that of **1**. Therefore, it should be expected that it would undergo reduction to the corresponding anion at potentials of **1** reduction (3). In other words, the electroreduction of **1** should follow the *ECE* mechanism (1-3).

(1)

(2)

(3)

However, taking into consideration the basicity of OH^- and $\mathbf{2}^-$ anions formed in reactions (2) and (3) and the acidic properties of the starting **1**, it can be assumed that the mechanism of its electroreduction would also involve protolytic equilibria (4)-(7). The results of calculations on the thermodynamics of these reactions shows that the equilibrium will be shifted to the right in all cases except (6) (Table 2). Nevertheless, earlier, insufficient attention was given to the effect of the specified reactions on the overall electroreduction mechanism. In the paper [71] dealing with electroreduction of methanol derivatives, the possibility of proton transfer between the starting compound and the products was not considered at all. The role of some mentioned reactions in the electroreduction mechanism of **1** derivatives was discussed in [73]. However, the conclusions on the general process scheme were made in [73] solely on the basis of a qualitative examination of CV curves and were mostly assumptions. Therefore, in order to determine reliably the mechanism of C-OH bond cleavage initiated by the electron transfer, it appeared expedient to study the kinetics of this process by electroanalytical methods. More generally, it may be interesting because in contrast to “real” selfprotonation reaction between initial anion radical and the starting molecule (*e.g.* [94]) there are not too many examples of proton transfer between starting molecule and the products of its anion radical dissociation [95-102].

(4)

(5)

(6)

(7)

3.2. Electrochemical Investigations

The figures demonstrate a CV curve (Fig. 3-5) and a current-potential curve of **1** electroreduction (Fig. 6) built from chronoamperometric data. The CV curves of **1** exhibit two cathodic peaks (Fig. 3). The potential of the second peak, corresponds to the electroreduction of **2**, which should be the product of *ECE* mechanism. As we might have expected based on the low activation energy of reaction (2), the electroreduction peak of **1** on CV curves in the range of potential scan rates studied (from 0.025 to 3 V·s⁻¹) is chemically irreversible and the anodic peak corresponding to **1**⁻ oxidation is not observed (Fig. 4). As noted above, it could be expected that electroreduction of **1** should be described by the *ECE* mechanism and the apparent number of electrons participating in electroreduction (n_{app}) should be 2. However, the n_{app} values found from CA data as the ratio of the limiting electroreduction current of **1** to the limiting current of an one-electron diffusion process, or in the case of CV as the ratio of the cathodic peak current to the peak current of a one-electron process not complicated by near-electrode reactions, are much smaller than 2. In the case of CA, in the range from 2 to 4 s, $n_{app} = 1.19 \pm 0.02$ and nearly does not depend on time and concentration of **1**. In the case of CV, the mean n_{app} value equals 0.98 ± 0.05 and does not depend on the depolarizer concentration, either. Such behavior corresponds to the achievement of pure kinetic conditions. This is not surprising, since the activation energy of the reaction (2) is extremely low, and the anions OH⁻ and **2**⁻ are highly basic.

The low n_{app} values allow us to assume that, along with reactions (1)-(3), reactions of the starting compounds with its electroreduction products also take place and lead to electrochemically inactive compounds. As noted above, it appears most likely that these reactions include the protonation of OH⁻ (4)-(5) and **2**⁻ anions (6)-(7). In favor of this hypothesis is the fact that the addition of equimolecular amount of phenol increases the peak current to a level corresponding to two electron *ECE* process.

At the same time the value of n_{app} for the mechanism (1)-(7) in pure kinetic conditions should be equal 2/3. Moreover, the CV curves do not show peaks that could be assigned to oxidation of carbon-centered (**1**⁻_C) or oxygen-centered anions (**1**⁻_O) of **1** (Fig. 5). The last feature of **1** electroreduction was already noted previously [73] and was explained by the reaction (8) of proton transfer between **1**⁻_C and **1**⁻_O to give neutral **1** and **3**²⁻. The peaks of **1**⁻ is also absent in the cyclic voltammograms of a solution of **1** which contains an equimolar amount of Bu₄NOH, although there are peaks corresponding to **3** and its dianion [82]

(8)

As comparison of CV curves for **1** and **3** shows, the curves of the former actually contain peaks of successive oxidation of **3**²⁻ and **3**⁻ (Fig. 4-5). Furthermore, we detected the formation of **3**²⁻ due to electroreduction of **1** upon preparative electrolysis of **1** at a limiting current

potential. Figure 5 shows the CV curves of the catholyte before and after the electrolysis. The initial part (from 0 to -0.4 V) of the last CV curve is not shown at the Fig. 5 because of considerable anode current corresponding to the oxidation of the $\mathbf{3}^{2-}$.

However, the results of quantum-chemical calculations for the thermodynamics of protolytic reactions involving $\mathbf{1}$ and its electroreduction products (Table 2) indicate that the equilibrium constant of proton transfer between $\mathbf{1}^-_{\text{C}}$ and $\mathbf{1}^-_{\text{O}}$ (8) is a few orders smaller than those for the dianion formation in reactions of OH^- with $\mathbf{1}^-_{\text{C}}$ and $\mathbf{1}^-_{\text{O}}$ (reactions 9 and 10).

(9)

(10)

Furthermore, one can see from Table 2 that the equilibrium constant of $\mathbf{3}^{2-}$ formation in the case of $\mathbf{1}^-_{\text{C}}$ (K_{10}) is close to the constant of $\mathbf{1}^-_{\text{C}}$ formation from a neutral molecule (K_4), whereas in the case of $\mathbf{1}^-_{\text{O}}$, K_9 is by 2 orders higher than K_5 , which explains the lack of oxidation peaks of C- or O- anions.

An experimental confirmation of an unusual ratio of equilibrium constants for reactions (5) and (9) was obtained by us previously [82]. For this purpose, we studied the protonation of cathodically generated $\mathbf{3}^{2-}$ (reactions 11-12) with water and determined the equilibrium constants of reverse reactions with respect to reactions (4-5) and (9-10). An advantage of this approach is that alcohol $\mathbf{1}$ is electrochemically inactive at potentials of $\mathbf{3}^{2-}$ formation, hence reactions (1)-(3) can be excluded from consideration. Therefore, we used a similar approach in this study in order to determine the parameters of protolytic equilibria (6)-(7) and (13)-(14).

(11)

(12)

(13)

(14)

As shown previously [82], two cathodic peaks are observed on the CV curves of $\mathbf{3}$ (Fig. 5), the first of which (-1.23 V) is related to $\mathbf{3}^{\cdot-}$ formation, whereas the second one (-1.87 V) corresponds to $\mathbf{3}^{2-}$ formation (curve *c*). The shape of the second peak indicates that it is of quasi-reversible nature that is observed for a number of electroreduction processes of anion radicals of carbonyl compounds to the corresponding dianions [103]. Comparison of experimental and theoretical cyclic voltammograms allowed us to estimate the heterogeneous constant of electron transfer rate: $k_{s, 12} = 0.01 \text{ cm}\cdot\text{s}^{-1}$. The low value of the constant may be caused by high energy of reorganization upon second electron transfer (the C-O bond length increases by 0.06 Å.). On the

anodic branch of the CV curve, peaks of $3^{\cdot-}$ (-1.16 V) и 3^{2-} (-1.76 V) anodic oxidation are observed.

Addition of **2** to a solution of **3** does not affect the current values corresponding to the formation and oxidation of $3^{\cdot-}$ even at a small potential scan rate ($0.025 \text{ V}\cdot\text{s}^{-1}$) and with a tenfold excess of **2**. This fact allows us to believe that **2** does not protonate $3^{\cdot-}$. On the other hand, the ratio of the anodic and cathodic branches of the second peak decreases with an increase in the concentration of **2** (Fig. 7, curves *b-d*). Furthermore, an anodic peak at -0.54 V corresponding to oxidation of fluorene anion 2^- appears in the presence of **2** (Fig. 7, curves *b-d*). It is of note that peaks of monoanions 1^-_C and 1^-_O do not appear on the CV curve of **3** (Fig. 7) upon addition of **2** (Fig. 7, curves *b-d*), like in the case of water addition [82]. Using the results of quantum-chemical calculations on the thermodynamics of 1^-_C and 2^- oxidation and the parameters of the correlation relationship [104], it can be concluded that the oxidation potential of 1^-_C should be about -0.3 V. However, no oxidation peaks are observed in this region (Fig. 7).

It should also be noted that the shapes of the cathodic and anodic peaks corresponding to the formation and oxidation of 3^{2-} on the CV curves of solutions containing a proton donor (Fig. 8) differ considerably from the shape typical of irreversible protonation of 3^{2-} and the 1^-_C and 1^-_O anions formed (Fig. 8, curve *c*). At the same time, the theoretical curves calculated for the mechanism (6)-(7) and (11)-(14) using the theoretical value $K_{15} = 15.4$ of the constant of equilibrium between the 1^-_C and 1^-_O anions and parameters listed in Section 2.2 (Fig. 7, curve *b*) have a shape similar to that observed experimentally.

(15)

The best fit between experimental and theoretical CV curves (Fig. 8, curves *a* and *b*) is reached at the ratio of constants K_{13}/K_6 and K_{14}/K_7 predicted on the basis of quantum-chemical calculations of the thermodynamics of the reactions in question (Table 2) but at the values of these constants approximately one to two orders lower than the theoretical ones. The latter fact may result from the use of the continual model to describe the solvation effects; however, this model does not account for the formation of hydrogen bonds with a solvent, which is typical of hydroxy derivatives. As shown below, the data obtained allowed us to give an adequate description of **1** electroreduction.

Thus, experimental results confirm the conclusion on the unusual ratio of constants, K_{13}/K_6 , made on the basis of quantum-chemical calculations. This ratio, like the unusual ratio of the equilibrium constants of reactions (5) and (9) that we found previously [82], is caused by a special feature of π^* -dianions, in particular, their lower basicity in comparison with other

negatively charged species [105], and can be observed in those cases where the corresponding protolytic equilibria give a π^* -dianion.

Unlike the electroreduction mechanism considered above at potentials of $\mathbf{3}^{2-}$ formation, the mechanism of $\mathbf{1}$ electroreduction, along with bulk reactions (4-5) and (8-10), should involve protonation of the fluorene anion formed, (6-7) and (13-14). Like in the previous case, the use of theoretical values of the ratio of equilibrium constants for the reactions mentioned above makes it possible to describe the electroreduction of $\mathbf{1}$ correctly in the entire range of concentrations and potential scan rates used. As one can see from Fig. 9, the shape of theoretical CV curves is in good agreement with the experimental curves of $\mathbf{1}$ electroreduction, and the experimental and theoretical peak currents are similar in the entire range of concentrations and potential scan rates:

$$i_p / i_p^{theor} = 1.06 \pm 0.09.$$

Comparison of the shape of experimental cyclic voltammograms with that of theoretical CV curves obtained by numeric simulation methods also allowed us to estimate the heterogeneous constant of electron transfer rate: $k_{s1} = 0.1 \text{ cm}\cdot\text{s}^{-1}$. The low value of the constant is apparently caused by high energy of reorganization upon electron transfer due to the fact that radical anion formation involves considerable structural changes. It should be noted that this constant has a similar value of $0.2 \text{ cm}\cdot\text{s}^{-1}$ in the case of N-(4-nitrophenyl)hydroxylamine [70], where formation of the radical anion is accompanied by elongation of the N-O bond by 0.03 \AA .

The electrolysis results also confirm the mechanism under discussion. The main products isolated from catholyte are $\mathbf{2}$ and $\mathbf{3}$. The yield of $\mathbf{3}$ is approximately equal to the theoretical value 50%, when the yield of $\mathbf{2}$ is about 20%. The decrease in the yield of $\mathbf{2}$ may be due to its homogeneous reduction by $\mathbf{3}^{2-}$ which gives rise $\mathbf{3}^{\cdot-}$ and $\mathbf{2}^{\cdot-}$. The contribution of this reaction should increase with increasing of $\mathbf{3}^{2-}$ and $\mathbf{2}$ concentrations. The formation of $\mathbf{3}^{\cdot-}$, which is reduced at the potential of electrolysis, explains why the initial decreasing of the current changes later for it growing. The presence of resin material among the products of the electrolysis (see 2.1) may be caused by the reactions of $\mathbf{2}^{\cdot-}$ and the products of its protonation.

4. Conclusion

The data of our experiments and calculations indicate that the electroreduction of fluorenol is accompanied by cleavage of the C-OH bond in its anion radical and by formation of bases, namely, fluorenol anion $\mathbf{2}^-$ and hydroxide anion OH^- , which participate in the protolytic equilibrium described by Scheme 2. The shift of equilibrium toward dianion formation is due to an unusual ratio of constants, $K_{II}/K_I \gg 1$, caused by a lower basicity of the π^* -dianion in comparison with other anions.

Conflict of interest

The authors declare that there is no conflict of interest with any financial organization regarding the material discussed in the manuscript.

Acknowledgements

Financial support of the Russian Science Foundation is acknowledged (RSF Grant 14-50-00126).

References

- [1] A. Houmam, *Chem. Rev.* 108 (2008) 2180. DOI: 10.1021/cr068070x
- [2] J.M. Saveant, *Adv. Phys. Org. Chem.* 35 (2000) 117. DOI: 10.1016/S0065-3160(00)35013-4
- [3] C.P. Andrieux, *Organic Electrochemical Mechanisms*, in *Encyclopedia of Analytical Chemistry*, Wiley Chichester (2000) 9983.
- [4] C.P. Andrieux, J.-M. Saveant, A. Tallec, R. Tardivel, C. Tardy, *J. Am. Chem. Soc.*, 119 (1997) 2420. DOI: 10.1021/ja963674b
- [5] R.J. Enemaerke, T.B. Christensen, H.Jensen, K.Daasbjerg, *J. Chem. Soc., Perkin Trans. 2*, (2001) 1620. DOI: 10.1039/B102835A
- [6] C.P. Andrieux, C. Combellas, F. Kanou., J.-M. Saveant, A. Thiebault, *J. Am. Chem. Soc.* 119 (1997) 9527. DOI: 10.1021/ja971094o
- [7] S. Antonello, F.J. Maran, *J. Am. Chem. Soc.* 120 (1998) 5713. DOI: 10.1021/ja9741180
- [8] S. Jakobsen, H. Jensen, S.U. Pendersen, K. Daasbjerg, *J. Phys. Chem. A* 103 (1999) 4141. DOI: 10.1021/jp990087e
- [9] J.M. Tanko, J.P. Phillips, *J. Am. Chem. Soc.* 121 (1999) 6078. DOI: 10.1021/ja990921d
- [10] T.A. Vaganova, E.V. Panteleeva, V.D Shteingarts, *Russ. Chem. Rev.* 77 (2008) 601. DOI: 10.1070/RC2008v077n07ABEH003776
- [11] H. Lund, *J. Electrochem. Soc.* 149 (2002) S21. DOI:10.1149/1.1462037
- [12] D.G. Peters, in *Organic Electrochemistry* (4th ed.), Marcel Dekker New York (2000) 341.
- [13] V.P. Ananikov, E.A. Khokhlova, M.P. Egorov, A.M. Sakharov, S.G. Zlotin, A.V. Kucherov, L.M. Kustov, M.L. Gening, N.E. Nifantiev, *Mendeleev Commun.* 25 (2015) 75. DOI: 10.1016/j.mencom.2015.03.001
- [14] J.S. Duca, M.H. Gallego, A.B. Pierini, R.A. Rossi, *J. Org. Chem.* 64 (1999) 2626. DOI: 10.1021/jo980657r
- [15] R.A. Rossi, A.B. Pierini, S.M. Palacios, in *Advances in Free Radical Chemistry*, Jai Press Singapore (1990) 193.
- [16] J.F. Bunnett, *Tetrahedron* 49 (1993) 4417. DOI: 10.1016/S0040-4020(01)81277-1

- [17] C. Costentin, P. Hapiot, M. Medebielle, J.-M. Saveant, *J. Am. Chem. Soc.*, 121 (1999) 4451. DOI: 10.1021/ja9902322
- [18] *Radical and Radical Ion Reactivity in Nucleic Acid Chemistry*, Ed. by M.M. Greenberg, John Wiley & Sons Hoboken New Jersey (2009).
- [19] A. Houmam, E.M. Hamed, *Chem. Commun.* 48 (2012) 11328. DOI: 10.1039/C2CC36835H
- [20] L.M. Bouchet, A.B. Penenory, M.Robert, J.E. Arguello, *RSC Adv.* 5 (2015) 11753. DOI: 10.1039/C4RA16154H
- [21] D.C. Magri, M.S. Workentin, *Molecules* 19 (2014) 11999. DOI: 10.3390/molecules190811999.
- [22] C.D. Stevenson, P.M. Garland, M.L. Batz, *J. Org. Chem.* 61 (1996) 5948. DOI: 10.1021/jo960645a
- [23] M.L. Batz, P.M. Garland, R.C. Reiter, M.D. Sanborn, C.D. Stevenson, *J. Org. Chem.* 62 (1997) 2045. DOI: 10.1021/jo9622082
- [24] T.A. Thoruton, G.A. Ross, D. Patil, *J. Am. Chem. Soc.* 111 (1989) 2434. DOI: 10.1021/ja00189a010
- [25] J.H. Wagenknecht, R.D. Goodin, P.J. Kinlen, F.E. Woodard, *J. Electrochem. Soc.* 131 (1984) 1559. DOI: 10.1149/1.2115909
- [26] J. Delaunay, M. Orlic-Le, J. Simonet, *J. Electrochem. Soc.* 142 (1995) 3613. DOI: 10.1149/1.2048387
- [27] M.G. Severin, M.C. Arevalo, F. Maran, E. Vianello, *J. Phys. Chem.* 97 (1993) 150. DOI: 10.1021/j100103a026
- [28] K. Daasbjerg, H. Jensen, R. Benassi, F. Taddei, S. Antonello, A. Gennaro, F. Maran, *J. Am. Chem. Soc.* 121 (1999) 1750. DOI: 10.1021/ja983374p
- [29] A.B. Meneses, S. Antonello, M.C. Arevalo, C.C. Gonzalez, J. Sharma, A.N. Walette, M.S. Workentin, F. Maran, *Chem. Eur. J.*, 13 (2007) 7983. DOI: 10.1002/chem.200700382
- [30] T.B. Christensen, K. Daasbjerg, *Acta. Chem. Scand.* 51 (1997) 307. DOI: 10.3891/acta.chem.scand.51-0307
- [31] S. Antonello, R. Benassi, G. Gavioli, F. Taddei, F. Maran, *J. Am. Chem. Soc.* 124 (2002) 7529. DOI: 10.1021/ja012545e
- [32] R.L. Donkers, F. Maran, D.D.M. Wayner, M.S. Workentin, *J. Am. Chem. Soc.* 121 (1999) 7239. DOI: 10.1021/ja9906148
- [33] S. Antonello, M. Musumeci, D.D.M. Wayner, F. Maran, *J. Am. Chem. Soc.* 119 (1997) 9541. DOI: 10.1021/ja971416o
- [34] M.S. Workentin, R.L. Donkers, *J. Am. Chem. Soc.* 120 (1998) 2664. DOI: 10.1021/ja974197f

- [35] R.L. Donkers, M.S. Workentin, *Chem. Eur. J.* 7 (2001) 4012. DOI: 10.1002/1521-3765(20010917)7:18<4012::AID-CHEM4012>3.0.CO;2-A
- [36] R.L. Donkers, M.S. Workentin, *J. Phys. Chem. B* 102 (1998) 4061. DOI: 10.1021/jp981457m
- [37] S. Antonello, F. Formaggio, A. Moretto, C. Toniolo, F. Maran, *J. Am. Chem. Soc.*, 123 (2001) 9577. DOI: 10.1021/ja010799u
- [38] D.C. Magri, M.S. Workentin, *Org. Biomol. Chem.* 6 (2008) 3354. DOI: 10.1039/B809356C
- [39] D.C. Magri, M.S. Workentin, *Chem. Eur. J.* 14 (2008) 1698. DOI:10.1002/chem.200701740
- [40] D.L. B. Stringle, D.C. Magri, M.S. Workentin, *Chem. Eur. J.* 16 (2010) 178. DOI: 10.1002/chem.200902023
- [41] F. Najjar, C. Andre-Barres, M. Baltas, C. Lacaze-Dufaure, D.C. Magri, M.S. Workentin, T. Tzedakis, *Chem. Eur. J.* 13 (2007) 1174. DOI: 10.1002/chem.200600445
- [42] R.L. Donkers, M.S. Workentin, *J. Am. Chem. Soc.*, 126 (2004) 1688. DOI: 10.1021/ja035828a
- [43] D.C. Magri, R.L. Donkers, M.S. Workentin, *J. Photochem. Photobiol. A* 138 (2001) 29. DOI:10.1016/S1010-6030(00)00386-5
- [44] D.C. Magri, M.S. Workentin, *Org. Biomol. Chem.* 1 (2003) 3418. DOI: 10.1039/B305348B
- [45] R.L. Donkers, J. Tse, M.S. Workentin, *Chem. Commun.* (1999) 135. DOI: 10.1039/A807795I
- [46] D.L.B. Stringle, R.N. Campbell, M.S. Workentin, *Chem. Commun.* (2003) 1246. DOI: 10.1039/B301909H
- [47] P. Maslak, T.M. Vallombroso, W.H. Chapman, J.N. Narvaez, *Angew. Chem., Int. Ed. Engl.* 33 (1994) 73. DOI: 10.1002/anie.199400731
- [48] A. Houmam, E.M. Hamed, P. Hapiot, J.M. Motto, A.L. Schwan, *J. Am. Chem. Soc.* 125 (2003) 12676. DOI: 10.1021/ja036710x
- [49] D.L.B. Stringle, M.S. Workentin, *Can. J. Chem.* 83 (2005) 1473. DOI: 10.1139/v05-164
- [50] P. Poizot, J. Simonet, *Electrochim. Acta* 56 (2010) 15. DOI: doi:10.1016/j.electacta.2010.09.020
- [51] A. Gennaro, A.A. Isse, C.L. Bianchi, P.R. Mussini, M. Rossi, *Electrochem. Commun.* 11 (2009) 1932. DOI: 10.1016/j.elecom.2009.08.021
- [52] M.A. Bhat, P.P. Ingole, V.R. Chaudhari, S.K. Haram, *J. Phys. Chem. B* 113 (2009) 2848. DOI: 10.1021/jp809749k
- [53] Y.-F. Huang, D.-Y. Wu, A. Wang, B. Ren, S. Rondinini, Z.-Q. Tian, C. Amatore, *J. Am. Chem. Soc.* 132 (2010) 17199. DOI: 10.1021/ja106049c
- [54] P. Du, D.G. Peters, *J. Electrochem. Soc.* 157 (2010) F167. DOI: 10.1149/1.3482019

- [55] V.A. Sauro, D.C. Magri, J.L. Pitters, M.S. Workentin, *Electrochim. Acta* 55 (2010) 5584. DOI: 10.1016/j.electacta.2010.04.080
- [56] L. Alvarez-Griera, I. Gallardo, G. Guirado, *Electrochim. Acta* 54 (2009) 5098. DOI: 10.1016/j.electacta.2009.02.037
- [57] M.A. Prasad, M.V. Sangaranarayanan, *Electrochim. Acta* 51 (2005) 242. DOI: 10.1016/j.electacta.2005.04.019
- [58] O. Scialdone, A. Galia, C. La Rocca, G. Filardo, *Electrochim. Acta* 50 (2005) 3231. DOI: 10.1016/j.electacta.2004.11.059
- [59] A.A. Isse, P.R. Mussini, A. Gennaro, *J. Phys. Chem. C* 113 (2009) 14983. DOI: 10.1021/jp904797m
- [60] C. Lagrost, S. Gmouh, M. Vaultier, P. Hapiot, *J. Phys. Chem. A* 108 (2004) 6175. DOI: 10.1021/jp049017k
- [61] J.S. Jaworski, P. Leszczynski, *J. Electroanal. Chem.* 464 (1999) 259. DOI: 10.1016/S0022-0728(99)00043-1
- [62] A.A. Isse, A. Galia, C. Belfiore, G. Silvestri, A. Gennaro, *J. Electroanal. Chem.* 526 (2002) 41. DOI: 10.1016/S0022-0728(02)00815-X
- [63] J.-M. Saveant, *Adv. Phys. Org. Chem.* 26 (1991) 1. DOI: 10.1016/S0065-3160(08)60044-1
- [64] H.M. Walborsky, C. Hamdouchi, *J. Am. Chem. Soc.* 115 (1993) 6406. DOI: 10.1021/ja00067a066
- [65] E. Peralez, J.C. Negrel, M. Chanon, *Tetrahedron* 51 (1995) 12601. DOI: 10.1016/0040-4020(95)00814-O
- [66] M. Chanon, *Molecules* 5 (2000) 289. DOI: 10.3390/50300289
- [67] N. Bodineau, J.-M. Mattalia, V. Thimokhin, K. Handoo, J.-C. Negrel, M. Chanon, *Org. Lett.* 2 (2000) 2303. DOI: 10.1021/ol006071k
- [68] V.A. Petrosyan, M.E. Niyazymbetov, *Russ. Chem. Rev.* 58 (1989) 644. DOI: 10.1070/RC1989v058n07ABEH003467
- [69] B. Soucaze-Guillous, H. Lund, *Acta Chem. Scand.* 52 (1998) 417. DOI: 10.3891/acta.chem.scand.52-0417
- [70] A.S. Mendkovich, M.A. Syroeshkin, D.V. Ranchina, M.N. Mikhailov, V.P. Gulytai, A.I. Rusakov, *J. Electroanal. Chem.* 728 (2014) 60. DOI: 10.1016/j.jelechem.2014.06.014
- [71] H. Lund, H. Doupeux, M.A. Michel, G.A. Mousset, J. Simonet, *Electrochim. Acta* 19 (1974) 629. DOI: 10.1016/0013-4686(74)85019-X
- [72] C. Nuntnarumit, F.M. Triebe, M. Dale Hawley, *J. Electroanal. Chem.* 126 (1981) 145. DOI: 10.1016/S0022-0728(81)80425-1

- [73] C. Nuntnarumit, M. Dale Hawley, *J. Electroanal. Chem.* 133 (1982) 57. DOI: 10.1016/0022-0728(82)87005-8
- [74] N. Ichinose, J. Hobo, S. Tojo, T. Majima, *Chem. Phys. Lett.* 330 (2000) 97. DOI: 10.1016/S0009-2614(00)01089-7
- [75] L. Nadjo, J.M. Saveant, *J. Electroanal. Chem. Interfacial Electrochem.*, 48 (1973) 113, DOI: 10.1016/S0022-0728(73)80300-6
- [76] C. Costentin, J.M. Saveant, *J. Electroanal. Chem.*, 564 (2004) 99. DOI: 10.1016/j.jelechem.2003.10.011
- [77] N. Leventis, X. Gao, *J. Electroanal. Chem.* 500 (2001) 78. DOI: 10.1016/S0022-0728(00)00263-1.
- [78] M.V. Mirkin, A.J. Bard, *Anal. Chem.* 64 (1992) 2293. DOI: 10.1021/ac00043a020.
- [79] N. A. Macias-Ruvalcaba, D. H. Evans, *J. Phys. Chem. B* 109 (2005) 14642. DOI: 10.1021/jp051641p.
- [80] N.G. Tsierkezos, *J. Solution. Chem.* 36 (2007) 289. doi: 10.1007/s10953-006-9119-9.
- [81] A.S. Mendkovich, M.A. Syroeshkin, L.V. Mikhailchenko, M.N. Mikhailov, A.I. Rusakov, V.P. Gul'tyai, *Internat. J. Electrochem.* 2011 (2011) 346043. DOI: 10.4061/2011/346043.
- [82] A.S. Mendkovich, M.A. Syroeshkin, M.N. Mikhailov, D.V. Ranchina, A.I. Rusakov, *Rus. Chem. Bull., Int. Ed.* 62 (2013) 1668. DOI: 10.1007/s11172-013-0242-7.
- [83] A.D. Becke, *J. Chem. Phys.*, 98 (1993) 5648. DOI: 10.1063/1.464913.
- [84] C. Lee, W. Yang, R.G. Parr, *Phys. Rev. B* 37 (1988) 785. DOI: 10.1103/PhysRevB.37.785.
- [85] S.H. Vosko, L. Wilk, M. Nusair, *Can. J. Phys.* 58 (1980) 1200. DOI: 10.1139/p80-159.
- [86] M.N. Mikhailov, N.D. Chuvylkin, I.V. Mishin, L.M. Kustov, *Russ. J. Phys. Chem. A* 83 (2009) 752. DOI: 10.1134/S0036024409050124.
- [87] Gaussian 03, Revision B.03, M. J. Frisch et al., Gaussian, Inc., Pittsburgh PA, 2003.
- [88] Gaussian 09, Revision A.02, M. J. Frisch et al., Gaussian, Inc., Wallingford CT, 2009.
- [89] J. Tomasi, M. Persico, *Chem. Rev.* 94 (1994) 2027. DOI: 10.1021/cr00031a013.
- [90] E. Cancès, B. Mennucci, J. Tomassi, *J. Chem. Phys.* 107 (1997) 3032. DOI: 10.1063/1.474659.
- [91] V. Barone, M. Cossi, *J. Phys. Chem. A* 102 (1998) 1995. DOI: 10.1021/jp9716997.
- [92] G. Scalmani and M. J. Frisch, *J. Chem. Phys.* 132 (2010) 114110. DOI: 10.1063/1.3359469.
- [93] N. Takeda, P.V. Poliakov, A.R. Cook, J.R.J. Miller, *J. Am. Chem. Soc.* 126 (2004) 4301. DOI: 10.1021/ja0389671
- [94] C. Amatore, G. Capobianco, G. Farnia, G. Sandona, J. M. Saveant, M.G. Severin, E. Vianello, *J. Am. Chem. Soc.* 107 (1985) 1815. DOI: 10.1021/ja00293a003

- [95] F. Maran, E. Vianello, F. D'Angeli, G. Cavicchioni, G. Vecchiati, J. Chem. Soc., Perkin Trans. 2 (1987) 33. DOI: 10.1039/P29870000033
- [96] F. Maran, M. Fabrizio, F. D'Angeli, E. Vianello, Tetrahedron 44 (1988) 2351. DOI: 10.1016/S0040-4020(01)81744-0
- [97] F. Maran, S. Roffia, M.G. Severin, E. Vianello, Electrochim. Acta 35 (1990) 81. DOI: 10.1016/0013-4686(90)85041-K
- [98] F. Maran, M.G. Severin, E. Vianello, Tetrahedron Lett. 31 (1990) 7523. DOI: 10.1016/S0040-4039(00)88535-4
- [99] M.L. Vincent, D.G. Peters, J. Electroanal. Chem., 344 (1993) 25. DOI: 10.1016/0022-0728(93)80044-I
- [100] G. Farnia, F. Marcuzzi, G. Sandona, J. Electroanal. Chem., 460 (1999) 160. DOI: 10.1016/S0022-0728(98)00370-2
- [101] A.B. Meneses, S. Antonello, M.C. Arevalo, F. Maran, Electrochim. Acta 50 (2005) 1207. DOI: 10.1016/j.electacta.2004.07.046
- [102] L. Preda, V. Lazarescu, M. Hillebrand, E. Volanschi, Electrochim. Acta 51 (2006) 5587. DOI: 10.1016/j.electacta.2006.02.032
- [103] A. René, D.H. Evans, J. Phys. Chem. C 116 (2012) 14454. DOI: 10.1021/jp3038335
- [104] M.A. Syroeshkin, M.N. Mikhailov, A.S. Mendkovich, A.I. Rusakov, Rus. Chem. Bull., Int. Ed. 58 (2009) 41. DOI: 10.1007/s11172-009-0006-6
- [105] L. Ebersson, Z. Blum, B. Helgée, K. Nyberg, Tetrahedron 34 (1978) 731. DOI:10.1016/0040-4020(78)88112-5

Figure Caption

Fig. 1. Profile of C-O bond dissociation in $1^{\cdot-}$ (DFT B3LYP/6-311++G(d,p) CSC-PCM)
 $\Delta G = G_2 - G_{OH}$.

Fig. 2. Variation of angle θ between the C9-H bond and the plane of the aromatic system along the coordinate of C-O bond dissociation reaction in $1^{\cdot-}$ (DFT B3LYP/6-311++G(d,p) CSC-PCM)

Fig. 3. CV curves for 5 mmol·L⁻¹ **1** and **2** in 0.1 M Bu₄NClO₄ in DMF at a potential scan rate of 0.1 V·s⁻¹.

Fig. 4. CV curves for 5 mmol·L⁻¹ **1** and **3** in 0.1 M Bu₄NClO₄ in DMF at a potential scan rate of 0.1 V·s⁻¹

Fig. 5. CV curves for 5 mmol·L⁻¹ solution of **1** before and after electrolysis, and 5 mmol·L⁻¹ solution of **3** in 0.1 M Bu₄NClO₄ solution in DMF at a potential scan rate of 0.1 V·s⁻¹.

Fig. 6. Currents on CA curves (in 2 s after applying an impulse) for 7.5 mmol·L⁻¹ **1** in 0.1 M Bu₄NClO₄ solution in DMF (circles) in comparison with a simulated curve (line).

Fig. 7. CV curves for 5 mmol·L⁻¹ solution of **3** in the absence (*a*, black) and in the presence of 5 mmol·L⁻¹ (*b*, blue), 10 mmol·L⁻¹ (*c*, red), and 26 mmol·L⁻¹ **2** (*d*, green) in 0.1 M Bu₄NClO₄ solution in DMF at a potential scan rate of 0.1 V·s⁻¹.

Fig. 8. CV curve of a mixture of 5 mmol·L⁻¹ **3** and 50 mmol·L⁻¹ **2** in 0.1 M Bu₄NClO₄ solution in DMF at a potential scan rate of 0.4 V·s⁻¹ (*a*, black), theoretical curves for mechanisms (6)-(7) and (11)-(14) (see Section 2.2 for simulation parameters) (*b*, blue), and (11)-(12) with irreversible protonation ($k_{\text{prot}} = 2 \cdot 10^2 \text{ M}^{-1} \cdot \text{s}^{-1}$) of **3**²⁻ (*c*, red).

Fig. 9. CV curve of 20 mmol·L⁻¹ **1** in 0.1 M Bu₄NClO₄ solution in DMF (—) in comparison with the theoretical curve (○) (see Section 2.2 for simulation parameters).

Scheme 1. Structures and designations of compounds and intermediates studied

Scheme 2. **Protolytic equilibrium between 1 and a base (B⁻ is a base).**

Table 1. Theoretical values of Gibbs free energy (DFT B3LYP/6-311++G(d,p) CSC-PCM)

Species	<i>G</i> , Kcal/mol
1	-361838
1 ^{-c}	-361533
1 ^{-o}	-361532
2	-314627
2 ⁻	-314320
2 [·]	-314235
3 ²⁻	-361228
OH ⁻	-47669
H ₂ O	-47981

Table 2. Theoretical values of the constants of protolytic equilibria. (DFT B3LYP/6-311++G(d,p) CSC-PCM)

Reaction	K
(4)	1.2E+05
(5)	4.9E+03
(6)	1.0E+00
(7)	2.4E+01
(8)	1.2E-01
(9)	9.8E+05
(10)	4.1E+04
(13)	2.0E+02
(14)	8.4E+00